Inorg. Chem. **2008**, *47*, 3634−3650

First-Principles Investigation of the Schrock Mechanism of Dinitrogen Reduction Employing the Full $HIPTN_3N$ Ligand

Stephan Schenk,[†] Boris Le Guennic,[‡] Barbara Kirchner,[§] and Markus Reiher*[,†]

Laboratorium für Physikalische Chemie, ETH Zürich, Wolfgang-Pauli-Strasse 10, CH-8093 Zürich, Switzerland, Laboratoire de Chimie, Ecole Normale Supérieure de Lyon, 46 Allée d'Italie, F-69364 Lyon Cedex 07, France, and Chair of Theoretical Chemistry, University of Leipzig, Linnestrasse 2, D-04103 Leipzig, Germany

Received October 20, 2007

In this work, we investigate with density functional methods mechanistic details of catalytic dinitrogen reduction mediated by Schrock's molybdenum complex under ambient conditions. We explicitly take into account the full $HIPTN_3N$ ligand without approximating it by model systems. Our data show that replacement of the bulky HIPT substituent by smaller groups leads to deviations in energy of up to 100 kJ mol^{-1}. Alternatives to the Chatt-like mechanism are also investigated. It turns out that for the generation of the first molecule of ammonia, protonation of the ligand plays a crucial role. With an increasing number of hydrogens on the terminal nitrogen atom, the reduction becomes more difficult. The energetically most feasible step is the generation of the first molecule of ammonia, while the preceding transfer of the second electron and proton is the most difficult one. Reaction energies are not only reported for decamethyl chromocene as in previous studies but also for a series of other metallocenes. Furthermore, results are provided in a way to allow for a convenient estimation of the thermochemical boundary conditions of catalysis with an arbitrary combination of acid and reductant. We demonstrate that the $[Mo](NNH_3)^+$ complex easily loses ammonia even in the absence of a reductant. For some complexes, spin states with higher multiplicity are the ground state instead of those with lower spin multiplicity.

1. Introduction

Nitrogen plays a very important role in life,[1] although its most abundant form, dinitrogen (N_2), is too inert for further processing and has to be converted to a more-active form, for instance, to ammonia; this process is called nitrogen fixation.[2] Nature accomplishes this task by means of nitrogenase enzymes.[1,3] However, these enzymes are not ubiquitous and are found only in some bacteria. On an industrial scale, ammonia is consumed in the production of fertilizers crucial for sustaining the world crop production. Ammonia is traditionally obtained by the Haber−Bosch process[4] through reaction of molecular nitrogen and hydrogen at elevated pressure and temperature mediated by heterogeneous catalysts. This process requires tremendous amounts of energy to catalytically transform inert dinitrogen to ammonia, and efficient catalysts working at mild conditions have been wanted by chemists for decades.[5,6]

As a result of these efforts, reduction of dinitrogen has been reported with a wide variety of metals,[7−19] but up to now, only two molybdenum complexes have proven to be

* To whom correspondence should be addressed. Email: markus.reiher@phys.chem.ethz.ch.
[†] Laboratorium für Physikalische Chemie, ETH Zürich.
[‡] Laboratoire de Chimie, Ecole Normale Supérieure de Lyon.
[§] Chair of Theoretical Chemistry, University of Leipzig.

(1) Rudolf, M.; Kroneck, P. M. H. In *Biogeochemical Cycles of Elements;* Sigel, A., Ed.; Metal Ions in Biological Systems, Vol. *43*; Taylor & Francis: Boca Raton, FL, 2005; Chapter 4, pp 75–103.
(2) Leigh, G. J., Ed. *Nitrogen Fixation at the Millenium*; Elsevier: New York, 2002.
(3) Noodleman, L.; Lovell, T.; Han, W.-G.; Li, J.; Himo, F. *Chem. Rev.* **2004**, *104*, 459–508.
(4) Holleman, A. F.; Wiberg, E.; Wiberg, N. *Lehrbuch der Anorganischen Chemie*, 101st ed.; de Gruyter: Berlin, 1995; Chapter 14, pp 645–649.
(5) Chatt, J.; Leigh, G. J. *Chem. Soc. Rev.* **1972**, *1*, 121–144.
(6) Schrock, R. R. *Philos. Trans. R. Soc. A* **2005**, *363*, 959–969.
(7) Himmel, H.-J.; Reiher, M. *Angew. Chem., Int. Ed.* **2006**, *45*, 6264–6288; *Angew. Chem.* **2006**, *118*, 6412–6437.
(8) Ohki, Y.; Fryzuk, M. D. *Angew. Chem., Int. Ed.* **2007**, *46*, 3180–3183; *Angew. Chem.* **2007**, *119*, 3242–3245.
(9) Chirik, P. J. *Dalton Trans.* **2007**, 16–25.
(10) Avenier, P.; Taoufik, M.; Lesage, A.; Solans-Monfort, X.; Baudouin, A.; de Mallmann, A.; Veyre, L.; Basset, J.-M.; Eisenstein, O.; Emsley, L.; Quadrelli, E. A. *Science* **2007**, *317*, 1056–1060.
(11) Yue, C.; Qiu, L.; Trudeau, M.; Antonelli, D. *Inorg. Chem.* **2007**, *46*, 5084–5092.

10.1021/ic702083p CCC: $40.75
Published on Web 03/22/2008

Scheme 1. [HIPTN$_3$N]Mo(N_2) Complex ([**Mo**](N_2))

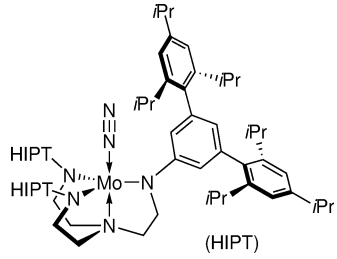

successful catalysts. The first system is that of Shilov et al. which forms mainly hydrazine with ammonia being only a minor product.[20] The other system is that of Schrock and co-workers, which has been shown to reduce dinitrogen to ammonia at ambient temperature and pressure in the presence of an electron and a proton source.[21]

In the active catalyst, the molybdenum is coordinated by a substituted trisamidoamine ligand (Scheme 1).[22–24] The best catalytic activity is achieved with a hexaisopropyl terphenyl substituent (HIPT) because it provides the best tradeoff between steric congestion of the metal center (to prevent dimerization) and accessibility of the active site. Replacement of the isopropyl groups by either methyl or *tert*-butyl leads to a dramatically reduced catalytic activity.[25] The terphenyl units are crucial too because substitution of one terphenyl group by phenyl ("hybrid ligands") leads to complexes that are no longer catalytically active.[26] Molybdenum appears to be unique in its catalytic capability because neither tungsten,[27] vanadium,[28] nor chromium[29] complexes with HIPTN$_3$N ligands are catalytically active.

In additon to the wealth of experimental results reported, quantum mechanical calculations have also contributed to the understanding of Schrock's catalytic cycle. In 2005, we performed extensive investigations of many variants of the trisamidoamine Mo complex including two of the huge, experimentally investigated chelate ligands.[30,31] We could demonstrate, for example, that simplified model systems are not appropriate for the understanding of *all* steps of the Schrock cycle by a quantum chemical approach.[30] Instead, substantial deviations in terms of reaction energies were found for small model complexes, which indicates that the huge chelate ligands do not only exert important steric effects but also modify the electronic structure at the reaction center so that the thermodynamics of the whole process are changed.[30,31] In a first communication on calculations employing the HIPTN$_3$N ligand, we investigated the ammonia−dinitrogen exchange reaction and studied the first proton transfer and reduction step.[31] In this full paper, we now present the complete analysis of all steps of the catalytic cycle employing the HIPTN$_3$N ligand. Next to experimental results, we follow side routes, such as the relative energetics of the three possible diazene isomers, to arrive at a complete picture of the capabilities of Schrock's catalyst. Another important aspect of this work is that the many experimental details known about the Schrock cycle allow us to better understand the reliability of quantum chemical calculations on metal-mediated catalysis, that is, quantum chemical calculations allow us to investigate any molecular structure, intermediate, charge, or spin state, but the results are always affected by unavoidable method-inherent errors that are difficult to assess and therefore hamper theoretical predictions of catalytic processes; recall, for instance, the difficulties that one faces with density functional theory (DFT) applied to transition-metal clusters, like the FeMo cofactor of Mo-nitrogenase (see, e.g., the reviews in refs 7, 32, and 33). Therefore, we also address in this work the question of the energetical boundary conditions for dinitrogen reduction if different acids and reductants are employed.

Computational studies on small *model* complexes conducted earlier in 2005 provide useful hints on how suitable the generic trisamidoamine Mo complex is for dinitrogen reduction and which effects are caused by the (full) HIPTN$_3$N ligand. Computations on very small model systems were performed by the group of Morokuma[34] in 2002, but it was Cao et al. who first investigated the *reaction* of a small model complex in which the HIPT substituents have all been replaced by phenyl groups.[35] However, because their study was performed in the context of nitrogenase activity, these authors did not use the proton and electron sources described by Schrock et al. but chose ammonium as the acid and an iron−sulfur cluster as the electron source. The full catalytic cycle as proposed by Schrock was investigated in a subsequent study by Studt and Tuczek who employed an even smaller model than Cao et al., where HIPT was simply

(12) Guillemot, G.; Castellano, B.; Prange, T.; Solari, E.; Floriani, C. *Inorg. Chem.* **2007**, *46*, 5152–5154.
(13) MacLachlan, E. A.; Hess, F. M.; Patrick, B. O.; Fryzuk, M. D. *J. Am. Chem. Soc.* **2007**, *129*, 10895–10905.
(14) Fryzuk, M. D.; Love, J. B.; Rettig, S. J.; Young, V. G. *Science* **1997**, *275*, 1445–1447.
(15) Vidyaratne, I.; Scott, J.; Gambarotta, S.; Budzelaar, P. H. M. *Inorg. Chem.* **2007**, *46*, 7040–7049.
(16) Zhou, M.; Jin, X.; Gong, Y.; Li, J. *Angew. Chem., Int. Ed.* **2007**, *46*, 2911–2914; *Angew. Chem.* **2007**, *119*, 2969–2972.
(17) Linnik, O.; Kisch, H. *Photochem. Photobiol. Sci.* **2006**, *5*, 938–942.
(18) Christian, G.; Stranger, R.; Yates, B. F.; Cummins, C. C. *Dalton Trans.* **2007**, 1939–1947.
(19) Hölscher, M.; Prechtl, M. H. G.; Leitner, W. *Chem.—Eur. J.* **2007**, *13*, 6636–6643.
(20) Shilov, A. E. *Russ. Chem. Bull., Int. Ed.* **2003**, *52*, 2555–2562.
(21) Yandulov, D. V.; Schrock, R. R. *Science* **2003**, *301*, 76–78.
(22) Schrock, R. R. *Acc. Chem. Res.* **2005**, *38*, 955–962.
(23) Weare, W. W.; Dai, X.; Byrnes, M. J.; Chin, J. M.; Schrock, R. R.; Müller, P. *Proc. Natl. Acad. Sci. U.S.A.* **2006**, *103*, 17099–17106.
(24) Yandulov, D. V.; Schrock, R. R. *J. Am. Chem. Soc.* **2002**, *124*, 6252–6253.
(25) Ritleng, V.; Yandulov, D. V.; Weare, W. W.; Schrock, R. R.; Hock, A. S.; Davis, W. M. *J. Am. Chem. Soc.* **2004**, *126*, 6150–6163.
(26) Weare, W. W.; Schrock, R. R.; Hock, A. S.; Müller, P. *Inorg. Chem.* **2006**, *45*, 9185–9196.
(27) Yandulov, D. V.; Schrock, R. R. *Can. J. Chem.* **2005**, *83*, 341–357.
(28) Smythe, N. C.; Schrock, R. R.; Müller, P.; Weare, W. W. *Inorg. Chem.* **2006**, *45*, 9197–9205.
(29) Smythe, N. C.; Schrock, R. R.; Müller, P.; Weare, W. W. *Inorg. Chem.* **2006**, *45*, 7111–7118.
(30) Le Guennic, B.; Kirchner, B.; Reiher, M. *Chem.—Eur. J.* **2005**, *11*, 7448–7460.
(31) Reiher, M.; Le Guennic, B.; Kirchner, B. *Inorg. Chem.* **2005**, *44*, 9640–9642.
(32) Reiher, M.; Hess, B. A. *Adv. Inorg. Chem.* **2004**, *56*, 55–100.
(33) Reiher, M. *Faraday Discuss.* **2007**, *135*, 97–124.
(34) Khoroshun, D. V.; Musaev, D. G.; Morokuma, K. *Mol. Phys.* **2002**, *100*, 523–532.
(35) Cao, Z.; Zhou, Z.; Wan, H.; Zhang, Q. *Int. J. Quantum Chem.* **2005**, *103*, 344–353.

substituted by hydrogen.[36] These authors used proton and electron abstraction reactions defined for isolated lutidinium and decamethyl chromocene $Cr(cp^*)_2$ as energetic reference for the protonation and reduction steps in the cycle. In 2006, Hölscher and Leitner[37] investigated the potential of the trisamidoamine Mo complex as catalyst for a direct reduction of dinitrogen to ammonia by molecular hydrogen with HIPT replaced by hydrogen as well. They found that for the hydrogenation reaction with H_2, the molybdenum complex is unsuitable. Much lower activation barriers were found when the molybdenum was replaced by either ruthenium or osmium. For the $HIPTN_3NRu$ system, they performed QM/MM calculations which employed the full HIPT ligand. However, they do not provide such data for molybdenum. The last quantum chemical study reported so far is that of Magistrato et al.[38] These authors use the full ligand, that is, the trisamidoamine chelate ligand with HIPT substituents only once for the calculation of the $HIPTN_3NMo(N_2)$ complex. For the investigation of the reaction energetics, they employ the same model as Cao et al., where HIPT is replaced by phenyl. Data is reported for lutidinium and $Cr(cp^*)_2$ as the proton and electron source.

This paper is organized as follows: We start with a detailed discussion of the reaction energetics for the electron/proton-transfer steps paying special attention to possible alternative reaction paths and continue with a closer look on the protonation steps. We then discuss complexation energies, compare net reaction energies with those of previous studies, and investigate the possible importance of states of different spin.

2. Computational Details

All calculations were carried out with the density functional programs provided by the Turbomole suite.[39] For all closed-shell electronic structures, we employed a restricted framework, while we switched to unrestricted Kohn−Sham calculations for the open-shell complexes. We used the Becke−Perdew exchange−correlation functional dubbed BP86[40,41] as implemented in Turbomole. Although it has been noted that reaction energies for dinitrogen activation may vary substantially with the choice of density functional,[42] we have demonstrated in our previous work[30] that for the complexes under investigation the differences between the hybrid B3LYP[43] and the BP86 functional are usually negligible in view of the general accuracy of DFT calculations. We therefore applied only the pure BP86 functional, for which we can invoke the efficient density-fitting resolution-of-the-identity (RI) techniques available in Turbomole. However, energy splittings between different spin states were calculated with our B3LYP* functional, which is a B3LYP functional with only 15% exact exchange admixture reparametrized for the energy splitting of states of different spin.[44–46]

For molybdenum and nitrogen we used Ahlrichs' valence triple-ζ TZVP basis set with polarization functions.[47] For the carbon and hydrogen atoms, we used the smaller split-valence plus polarization functions (SVP) basis set.[48] The corresponding RI auxiliary basis sets were taken from the Turbomole library. For the molybdenum atom, an effective core potential (ECP) from the Stuttgart group was applied.[49] This ECP also guarantees a reasonable modeling of scalar-relativistic effects on molybdenum.

All molecular structures were fully optimized until the length of the gradient vector had approached about 0.001 au, and the energetical difference of the last twenty structures in the optimization procedure was below 1 kJ mol^{-1}. Consequently, we mainly report rounded energies in kJ mol^{-1} without decimal places. We tested various arrangements of the sterically demanding chelate ligand to arrive at an optimum conformation. All further structures were optimized starting from this pre-optimized arrangement to reduce conformational effects on the reaction energetics to a minimum. We should emphasize that the complexes under investigation comprise about 280 atoms which were all treated explicitly (with the exception of the core electrons of the molybdenum that were replaced by the ECP).

The basis set superposition error of the TZVP basis set with respect to coordination energies amounts to about 10 kJ mol^{-1} (see, for instance, ref 50) and is therefore negligible for the discussion of coordination energies of N_2 or NH_3, especially in view of the fact that we are interested in reaction energy *differences*, where basis set superposition effects cancel to a large extent. If not mentioned otherwise, all energies are given for the species with the lowest spin and have not been corrected for basis set superposition effects and the zero-point vibrational energy.

Population analyses according to Mulliken and Löwdin have been performed with our local version of the Moloch module of Turbomole.[51] For open-shell systems, the natural orbitals as constructed by Turbomole were used. Hydrogen bond energies were estimated with the shared-electron-numbers (SEN) method using a slope for the relation between interaction energy and two-center-shared-electron number of −354 kJ mol^{-1}.[52,53]

Molecular structure representations were created with the program Molden.[54]

3. Results and Discussion

Most reaction steps involved in the reduction of dinitrogen coordinated to a trisamidoamine Mo complex require the transfer of electrons and protons. Hence, positive and

(36) Studt, F.; Tuczek, F. *Angew. Chem., Int. Ed.* **2005**, *44*, 5639–5642.
(37) Hölscher, M.; Leitner, W. *Eur. J. Inorg. Chem.* **2006**, 4407–4417.
(38) Magistrato, A.; Robertazzi, A.; Carloni, P. *J. Chem. Theory Comput.* **2007**, *3*, 1708–1720.
(39) Ahlrichs, R.; Bär, M.; Häser, M.; Horn, H.; Kölmel, C. *Chem. Phys. Lett.* **1989**, *162*, 165–169.
(40) Becke, A. D. *Phys. Rev. A: At., Mol., Opt. Phys.* **1988**, *38*, 3098–3100.
(41) Perdew, J. P. *Phys. Rev. B: Condens. Matter Mater. Phys.* **1986**, *33*, 8822–8824.
(42) Graham, D. C.; Beran, G. J. O.; Head-Gordon, M.; Christian, G.; Stranger, R.; Yates, B. F. *J. Phys. Chem. A* **2005**, *109*, 6762–6772.
(43) Becke, A. D. *J. Chem. Phys.* **1993**, *98*, 5648–5652.
(44) Reiher, M.; Salomon, O.; Hess, A. B. *Theor. Chem. Acc.* **2001**, *107*, 48–55.
(45) Reiher, M. *Inorg. Chem.* **2002**, *41*, 6928–6935.
(46) Salomon, O.; Reiher, M.; Hess, B. A. *J. Chem. Phys.* **2002**, *117*, 4729–4737.
(47) Schäfer, A.; Huber, C.; Ahlrichs, R. *J. Chem. Phys.* **1994**, *100*, 5829–5835.
(48) Schäfer, A.; Horn, H.; Ahlrichs, R. *J. Chem. Phys.* **1992**, *97*, 2571–2577.
(49) Andrae, D.; Häussermann, U.; Dolg, M.; Stoll, H.; Preuss, H. *Theor. Chim. Acta* **1990**, *77*, 123–141.
(50) Reiher, M.; Hess, B. A. *Chem.—Eur. J.* **2002**, *8*, 5332–5339.
(51) Herrmann, C.; Reiher, M.; Hess, B. A. *J. Chem. Phys.* **2005**, *122*, 034102.
(52) Reiher, M.; Sellmann, D.; Hess, B. A. *Theor. Chem. Acc.* **2001**, *106*, 379–392.
(53) Thar, J.; Kirchner, B. *J. Phys. Chem. A* **2006**, *110*, 4229–4237.
(54) Schaftenaar, G.; Noordik, J. H. *J. Comput.-Aided Mol. Des.* **2000**, *14*, 123–134.

negative charges are generated stepwise. However, the quantum chemical description of reactions that generate charged species inevitably results in huge reaction energies because of the fact that a cationic species features a significantly lower absolute energy than its neutral parent having the same number of electrons (but a different number of protons). On the other hand, the addition of electrons to a (large) molecule with constant and spatially fixed number of protons decreases the total energy as well if the electron is truly bound by the molecule.

Consequently, proton affinities (and to a smaller extent also electron affinities) of isolated species (as found in the gas phase) tend to become as large as 1000 kJ mol^{-1}. In homogeneous phase, one may expect that the charges are compensated by a dielectric surrounding, which would reduce the energetic stabilization of the cation so that the calculated proton affinity takes a smaller, more convenient numerical value. For this reason, dielectric continuum models are often used in quantum chemical calculations to avoid disturbingly large reaction energies (see, e.g., ref. 36). But such continuum models introduce many new model-dependent parameters whose role on the modeled reactions is not as clear as one may hope. Certainly, the resulting energies for reactions that involve charged particles then seem to be more reasonable, but it is not clear how a chosen continuum model may affect the reaction energy. In the special case of dinitrogen reduction studied here, we also note that the reactions are carried out in an apolar alkane solution so that dielectric continuum effects are expected to play a minor role.

For these reasons, we employ a different protocol here. First of all, we prefer to give the *intrinsic* reaction energies of the isolated system. Although this might partly result in large reaction energies, this approach allows us to discuss the intrinsic effects of the isolated system to be extracted from a thoughtful analysis of the much smaller differences of large absolute reaction energies. For the discussion of possible reaction paths only these relative effects are important. After a complete analysis of the intrinsic effects, we then study a one-pot model for selected reaction steps, in which the catalyst plus acid are treated as an isolated system in the quantum chemical calculation so that we avoid the production of charged species. It should be emphasized that both approaches do not require the tuning of dielectric effects in order to arrive at chemically reasonable reaction energies.

For the Lewis-type structure formulas in the following schemes, we chose reasonable resonance structures. We want to point out that a clear location of charges is impossible because the population analyses (see Computational Details) show no clear trends because of significant varying delocalization effects. The charges assigned to particular atoms are thus formal charges and must not be overemphasized. We do not discuss the optimized structures in detail (because the coordinates will be given as Supporting Information and can also be obtained from the authors and because we included such a discussion already in our earlier papers).[30,31] Instead, we ensured that the Lewis-type structures in the schemes to follow represent a good qualitative picture of the result of the structure optimization regarding the nitrogen species to be reduced.

Table 1. Intrinsinc Ionization Energy (IIE) and Idealized Spin Quantum Numbers (S) of the Ground State for Some Metallocenes (RI-BP86/TZVP)[a]

reductant	IIE (kJ mol^{-1})	S^{neutral}	S^{cation}
$Cr(cp)_2$	+539.1	1.0	1.5
$Cr(cp^*)_2$	+485.1	1.0	1.5
$Fe(cp)_2$	+648.6	0.5	1.0
$Fe(cp^*)_2$	+561.0	0.5	1.0
$Co(cp)_2$	+504.2	0.5	0.0
$Co(cp^*)_2$	+439.5	0.5	0.0
$Ni(cp)_2$	+593.1	1.0	0.5
$Ni(cp^*)_2$	+477.6	1.0	0.5

[a] cp = cyclopentadiene; cp* = pentamethyl cyclopentadiene.

3.1. Electron- and Proton-Donation Reactions. Electrons required for the reduction are provided by the oxidation of a reductant. Experimentally, metallocenes have been employed for this purpose. Calculated intrinsic ionization energies for some metallocenes M

$$M \rightarrow M^+ + e^- \qquad (1)$$

are given in Table 1. Note that in this approach the released electron leaves the system with zero energy so that all ionization energies are identical to the energy difference of the cationic and the neutral metal complex. Among the metallocenes are $Cr(cp^*)_2$, $Co(cp)_2$, and $Co(cp^*)_2$ which were applied experimentally.[55] The intrinsic ionization energy (IIE) thus corresponds to the energy required to detach an electron from an isolated metallocene. As discussed above, the intrinsic ionization energies appear to be large and positive, but only their relative magnitudes are to be considered decisive. Consequently, we immediately understand from the IIE that, for example, decamethyl chromocene is, in accordance with experiment, a strong reductant when we compare its IIE of +485.1 kJ mol^{-1} with the larger energies required for the ionization of the two ferrocenes. For all complexes we calculated the total energies for the spin states that are lowest in energy (see Table 1). The RI-BP86/TZVP calculations reproduce the same order in the energy of the spin states as was reported in the literature.[46,56]

The acid that is commonly applied as a proton source is a 2,6-dimethylpyridinium (lutidinium, Lu) salt. For the present discussion, we deemed the influence of the very bulky borate counterion to be neglibile and did not include it in the calculations. The released proton is considered to be at rest (like the electron in case of the reductant before) so that the proton affinity is calculated from the cationic acid and neutral base only. Then, the energy required to abstract the N-bound proton from lutidinium is calculated to be 1000.2 kJ mol^{-1}. This huge value seems to be contradictory to the fact that lutidinium is an acid. However, one should keep in mind that this value corresponds to the energy required for proton abstraction from the isolated system in vacuum. Since all other proton affinities are also calculated as intrinsic proton affinities, the relative energies are then chemically meaningful and lutidinium features the smallest intrinsic proton affinity.

(55) Yandulov, D. V.; Schrock, R. R. *Inorg. Chem.* **2005**, *44*, 1103–1117.
(56) Elschenbroich, C.; Salzer, A., *Organometallics*, 2nd ed.; VCH: Weinheim, Germany, 1992; Chapter 15, p 321.

Scheme 2. Possible Reaction Paths for the First Proton- and Electron-Transfer onto Coordinated N_2[a]

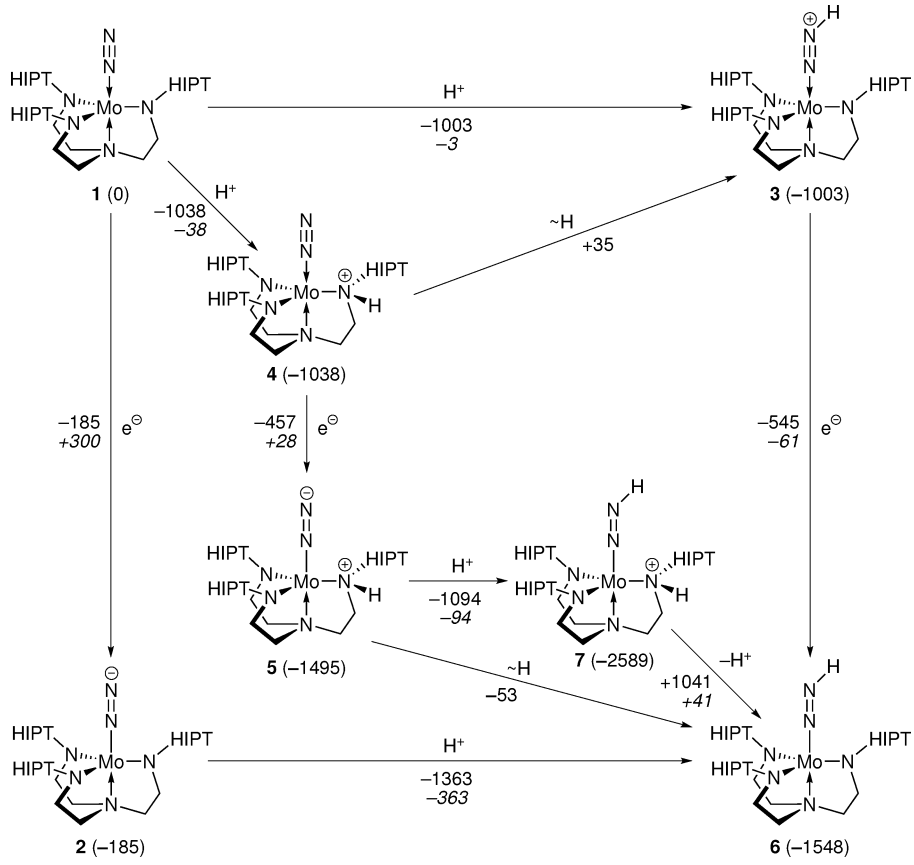

[a] Energies are given in kJ mol^{-1}. Values in *italics* correspond to the reaction energies obtained with lutidinium or $Cr(cp^*)_2$, respectively.

After having introduced the basic modeling approaches and the resulting intrinsic ionization energies and intrinsic proton affinities, we now proceed to discuss the proton- and electron-transfer steps onto dinitrogen bound to the trisamidoamine Mo complex.

3.2. Transfer of the first electron/proton pair. The *first* proton−electron transfer onto dinitrogen coordinated end-on to the molybdenum complex can be considered a very important step because it generates the first activated "N_2" species. This first reduction step of [**Mo**](N_2) (**1**), where [**Mo**] is a short-hand notation for [HIPTN_3N]Mo, has already been discussed in part in a previous communication.[31] We briefly recall these results to elaborate on them. In principle, three distinct reaction paths are possible (Scheme 2). The [**Mo**](N_2) complex **1** can be either reduced first or protonated first. The results in Scheme 2 shows that reduction of **1** to **2** is exothermic by −185 kJ mol^{-1}. However, as can be seen from Table 1, the accompanying oxidation of the reducing agent requires much more energy. This renders the overall reaction quite endothermic for all metallocenes in Table 1. Thus, an initial reduction step appears to be rather unlikely.

Instead, for simple electrostatic reasons, protonation of the [**Mo**](N_2) complex prior to reduction is favored. The seemingly strong exothermicity of the protonation is counterbalanced by the fact that proton abstraction from the 2,6-dimethylpyridinium (lutidinium, Lu) cation requires 1000.2 kJ mol^{-1}. Therefore, protonation of the N_2 moiety in **1** yielding **3** is essentially thermoneutral, while protonation of the ligand resulting in **4** is slightly exothermic. Thus, from a thermodynamical point of view, protonation of the ligand is the preferred reaction path in the first step.

The addition of a second proton at the terminal N of the N_2 moiety (−750 kJ mol^{-1}) or at another ligand amide group (−785 kJ mol^{-1}) of **4** is much less exothermic (data not shown) than the first protonation. This is quite reasonable because the complex already bears a positive charge that should result in a reduced electron density at the active site and therefore strongly disfavor addition of another proton to it. Thus, with lutidinium as the acid, these reactions would be endothermic by more than 200 kJ mol^{-1} and are therefore clearly not important pathways under the reaction conditions usually applied. However, if extremly strong acids were used, these reactions might become important.

In principle, an oxidative addition of a proton to the central molybdenum atom under generation of a hydride could be an alternative route for the first H-transfer step. But this was not observed in our calculations because we were unable to locate such a structure on the potential energy hypersurface. During the structure optimization process, the proton always inadvertently moved to a nearby amide nitrogen of the HIPT ligand. We therefore assume that such hydride structures do not play a role in the catalytic cycle.

Instead, the first protonation step is followed by a reduction. From Scheme 2 and Table 1, one can see that the reduction of **4** resulting in **5** is energetically almost neutral with either $Cr(cp^*)_2$ or $Co(cp^*)_2$ but becomes endothermic

Scheme 3. Possible Reaction Paths for the Transfer of a Second Electron−proton Pair onto the [**Mo**](NNH) Moiety[a]

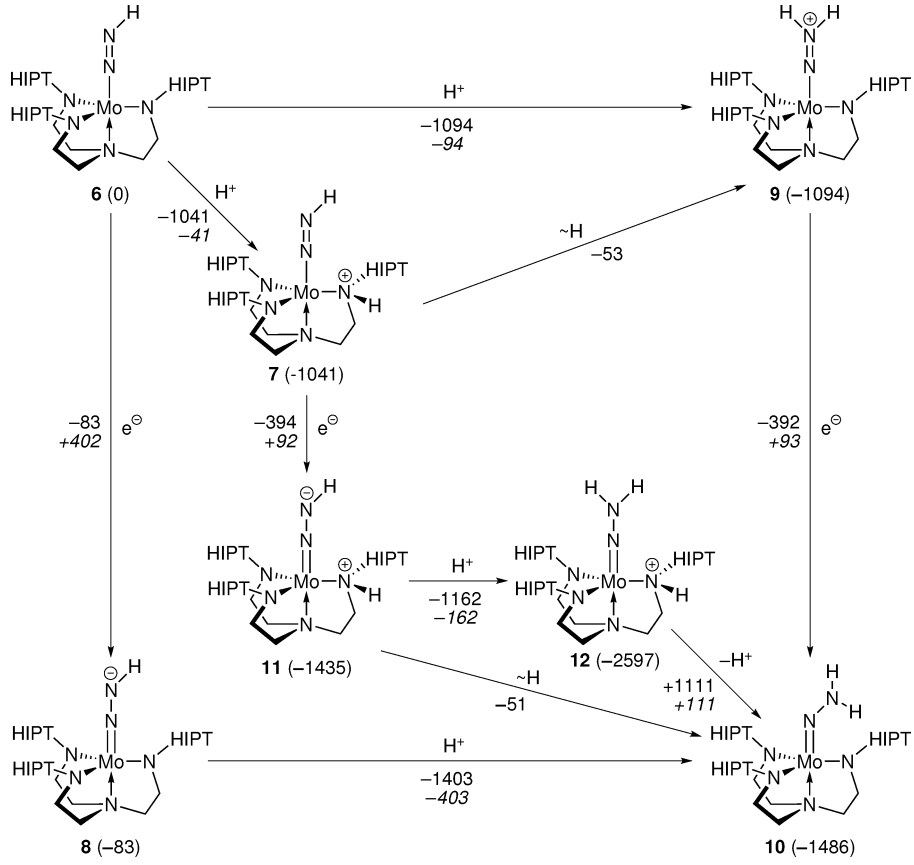

[a] Energies are given in kJ mol^{-1}. Values in *italics* correspond to the reaction energies obtained with lutidinium or Cr(cp*)$_2$, respectively.

with weaker reductants such as Fe(cp)$_2$. In addition, as we will show below in the discussion of the one-pot model, the intrinsic electron affinity is calculated too high because of an overstabilization of the solvation-free protonated complexes resulting from the uncompensated positive excess charge. Therefore, slightly endothermic reduction steps with Cr(cp*)$_2$, for example reaction from **4** to **5**, are not problematic and should not be overemphasized. Naturally, this also holds for later steps in the catalytic cycle.

The reduction of **3** to **6** is more exothermic than reduction of **4** to **5**. But this overall path is less likely than the one involving **4** because the latter is energetically favored over **3**. Furthermore, protonation of **5** yielding **7** is quite exothermic (more than 90 kJ mol^{-1} with lutidinium). As one might expect, the proton transfer onto the N_2 moiety in **5** is more exothermic and thus more feasible than that onto **1**. In the discussion of the one-pot model below, we will demonstrate that kinetic aspects can be safely ignored for the protonation reactions and thus the reasoning based solely on thermodynamics is justified.

The last step in the formation of the [**Mo**](NNH) complex **6** comprises deprotonation of the ligand. This process, however, is endothermic (41 kJ mol^{-1} with lutidinium) and thus slightly disfavored. Within the accuray of the applied density functional method, the energies associated with protonation of **1** and **6** are indistinguishable. Thus, the energy gained by formation of **4** may still be available to afford deprotonation of **7** to a certain degree. Therefore, **6** may be present in minute amounts but the equilibrium is strongly shifted toward **7**.

The reaction sequence **5**−**7**−**6** can be interpreted in terms of an intermolecular proton transfer from the ligand nitrogen atom onto the N_2 moiety. Alternatively, as indicated in Scheme 2, this isomerization could also occur in an intramolecular fashion. The corresponding reaction energy is negative and thus this process is feasible from a thermodynamical point of view.

Finally, we should note that the energy difference between **1** and **6** is −1548 kJ mol^{-1} because we have formally added a hydrogen radical whose energy is exactly known to be 0.5 hartree atomic units, that is, −1312.8 kJ mol^{-1}.

3.3. Transfer of the Second Electron/Proton Pair. As discussed in the previous section, the [**Mo**](NNH) complex (**6**) is considered to be present only in tiny amounts. Its direct reduction to **8** (Scheme 3) is even more endothermic than that of **1** and is thus clearly not an important pathway on the potential energy surface. Therefore, as in the previous step, protonation is required prior to reduction.

In contrast to the transfer of the first proton (Scheme 2), protonation of the terminal NH group resulting in **9** is now preferred by more than 50 kJ mol^{-1} over ligand protonation (Scheme 3). In principle, the proton could either be transferred directly from the ligand to the NNH moiety or by a base-assisted deprotonation/reprotonation mechanism (luti-

Scheme 4. Lewis Structure Representation of the Three Different Isomers of [**Mo**](N_2H_2)

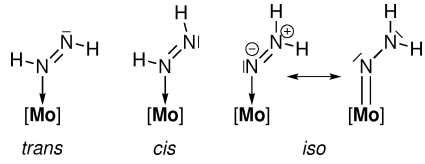

dine is always present under experimental conditions). Especially the latter base-mediated tautomerism should also be feasible kinetically.[57–60] We therefore may assume that **9** can be formed from **7**, possibly involving the neutral species **6**.

The energy gained upon reduction of either **7** or **9** is essentially the same. The reduction is therefore independent of the position of the extra proton and will not discriminate between both possible reaction paths. The transfer of the second electron appears to be more difficult than that of the first one; the electron affinity of **7** is more than 60 kJ mol^{-1} less negative than that of **4**.

The particular reaction path for the formation of **10** depends on whether **7** can be reduced to **11** before **7** undergoes isomerization to **9**. If reduction is fast enough, **11** will be formed. Because of the negative charge on its terminal NH group, protonation of **11** yielding **12** is very favorable ($\Delta E = -162$ kJ mol^{-1} with lutidinium as acid). If, on the other hand, reduction of **7** is slow, it will isomerize to **9** which in turn can be reduced to **10**. However, the [**Mo**](NNH_2) complex **10** can very easily be protonated at one of the ligand's nitrogen atoms. Like in the case of the [**Mo**](NNH) complex **6**, it will therefore be present also only in minute amounts.

The NNH_2 ligand in **10** is not planar with a HNNH dihedral angle of about 146°. It can be regarded as an hydrazido or *iso*-diazene moiety coordinating to the molybdenum center (Scheme 4). Since it is known from both experiment[61,62] and theory[63,64] that the trans isomer of diazene is the most stable one, this instantaneously raises the question whether other isomers of **10** can become important intermediates in the Schrock cycle as well. We therefore also investigated complexes with a *cis*- and *trans*-diazene ligand. Surprisingly, these complexes are calculated to be only 17.4 kJ mol^{-1} (trans) and 38.2 kJ mol^{-1} (cis) higher in energy than **10**. The end-on coordinated *iso*-diazene naturally evolves from the protonation−reduction steps of Scheme 3, that is, to bind a second proton to the terminal nitrogen atom of N_2 is most likely in this linear arrangement (despite of the fact that the isolated *iso*-diazene ligand is the most unfavorable one). But the energetically close lying trans and cis isomers suggest that **10** can rearrange.

While the iso arrangement is quite unfavorable for isolated diazene, the high electron density on the negatively charged nitrogen atom renders it a very good electron-donating ligand. Quantitative evidence for this rather qualitative statement is provided further below in the discussion of complexation energies.

3.4. Transfer of the Third Electron/Proton Pair. Transfer of the third electron−proton pair leads to formation of the first ammonia molecule (Scheme 5). As discussed above, protonation of the [**Mo**](NNH_2) complex **10** to give **12** is very favorable. In contrast to the results of the previous section, an isomerization of **12** to **13** is unlikely because the latter is disfavored by more than 70 kJ mol^{-1}. A direct reduction of the [**Mo**](NNH_2) complex **10** to **14** is unlikely under experimental reaction conditions. The electron affinity of **10** is positive and thus reducing agents much stronger than the experimentally applied metallocenes would be required.

The most-feasible route appears to be reduction of the [**Mo**](NNH_2) complex with a protonated ligand (**12**) under formation of **15**. The overstabilization of an isolated protonated complex leads to an underestimation of the intrinsic reaction energy for the reduction. Subsequent protonation at N^{β} would lead to a compound where a neutral ammonia molecule binds to the nitrogen atom of a metal nitride, a very unfavorable bonding situation. Instead, as soon as a proton approaches the N^{β} atom of the NNH_2 moiety in **15**, the N−N bond is cleaved, and ammonia begins to leave. No barrier is associated with this process (see below). Upon subsequent deprotonation of the ligand, the nitrido species **16** is formed. We should recall that such nitrido species are well-known for molybdenum complexes.[65,66]

Protonation at N^{α} in **15** would open up a side-reaction channel leading to formation of hydrazine. Although this proton transfer is exothermic by approximately 150 kJ mol^{-1} with lutidinium, it is still thermodynamically less favorable than protonation at N^{β} because the latter eventually will yield products 200 kJ mol^{-1} more stable than **15**. This is further corroborated by the fact that hydrazine has never been observed experimentally.[22]

Formation of ammonia under cleavage of the N−N bond immediately occurs upon either reduction of **13** or protonation of **14**. This is evident from the fact that we were unable to locate a single complex with a neutral N_2H_3 moiety on the potential energy surface; ammonia always spontaneously dissociates from the complex upon structure optimization as described already in our previous work on the Schrock catalyst.[30,31] Magistrato et al. confirm the barrierless dissociation of ammonia suggested in refs 30 and 31 on the basis of molecular dynamics simulations.[38] It should be noted

(57) Li, P.; Bu, Y. *J. Phys. Chem. B* **2004**, *108*, 18088–18097.
(58) Tautermann, C. S.; Loferer, M. J.; Voegele, A. F.; Liedl, K. R. *J. Phys. Chem. B* **2003**, *107*, 12013–12020.
(59) Liao, R.-Z.; Ding, W.-J.; Yu, J.-G.; Fang, W.-H.; Liu, R.-Z. *J. Phys. Chem. A* **2007**, *111*, 3184–3190.
(60) Delchev, V. B.; Shterev, I. G.; Mikosch, H.; Kochev, N. T. *J. Mol. Model.* **2007**, *13*, 1001–1008.
(61) Backa, R. A.; Willis, C.; Ramsay, D. A. *Can. J. Chem.* **1974**, *52*, 1006–1012.
(62) Sellmann, D.; Hennige, A. *Angew. Chem., Int. Ed.* **1997**, *36*, 276–278; *Angew. Chem.* **1997**, *109*, 270–271.
(63) Pople, J. A.; Curtiss, L. A. *J. Chem. Phys.* **1991**, *95*, 4385–4388.
(64) Reiher, M.; Salomon, O.; Sellmann, D.; Hess, B. A. *Chem.—Eur. J.* **2001**, *7*, 5195–5202.
(65) Dehnicke, K.; Strähle, J. *Angew. Chem., Int. Ed.* **1992**, *31*, 955–978; *Angew. Chem.* **1992**, *104*, 978–1000.
(66) Dehnicke, K.; Strähle, J. *Angew. Chem., Int. Ed.* **1981**, *20*, 413–426; *Angew. Chem.* **1981**, *93*, 451–464.

Scheme 5. Possible Reaction Paths for the Transfer of the Third Electron and Proton and Formation of the First Ammonia Molecule[a]

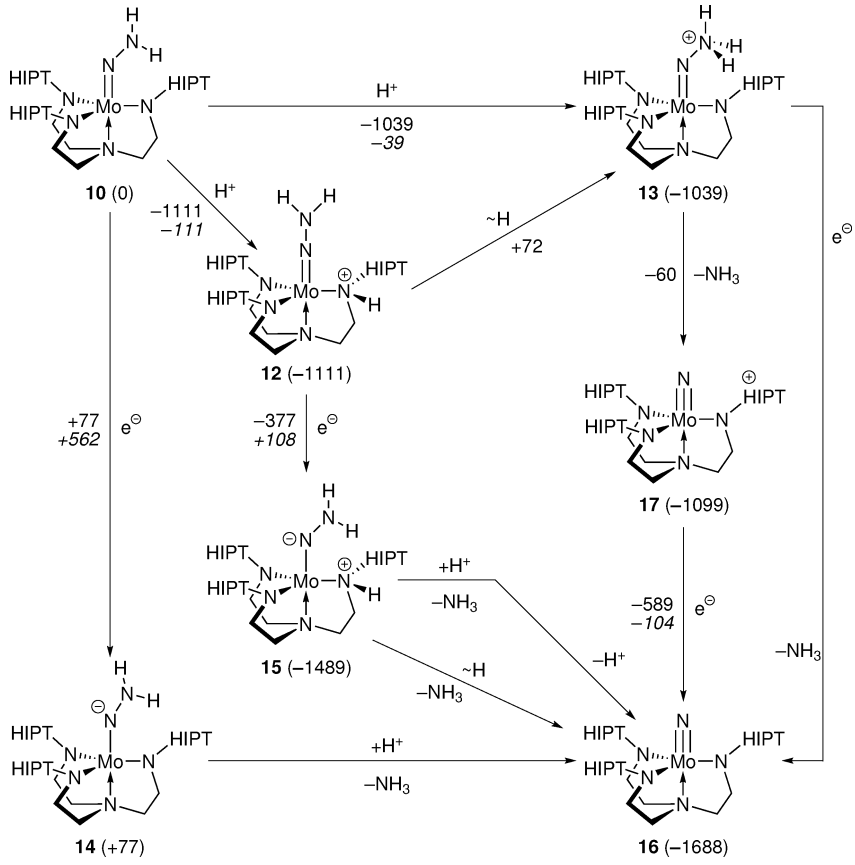

[a] Complexes with a neutral NH_3 moiety are unstable and immediately loose ammonia. Energies are given in kJ mol^{-1}. Values in *italics* correspond to the reaction energies obtained with lutidinium or Cr(cp*)$_2$, respectively.

that the assignment of a bond energy to the N−N bond in [**Mo**](NNH$_3$) through the definition of a net reaction like

$$\mathbf{13} + \text{reductant} \rightarrow \mathbf{16} + NH_3 + \text{reductant}^+ \qquad (2)$$

as done in ref 36 would be completely misleading because the only energy that is calculated is the electron affinity of the reductant, that is, the choice of different reductants would yield different N−N bond energies for the same molecule, which would be meaningless.

Because of the unfavorable protonation at the terminal N (with respect to **12**), the [**Mo**](NNH$_3$)$^+$ complex (**13**) should only be generated in minute amounts. Furthermore, the HIPT substituents seem to be crucial for the stability of the (NNH$_3$)$^+$ moiety because similar attempts to locate such a structure invariantly failed if HIPT was replaced by either hydrogen or methyl. Single-point energy calculations at different N−N bond distances show that the dissociation of ammonia from **17** itself is essentially thermoneutral thus indicative of a very weak binding of ammonia in **13**. Relaxation of the [**Mo**](N)$^+$ fragment left behind once ammonia has dissociated yields an overall reaction energy for the dissociation of −60 kJ mol^{-1}. For N−N bond distances between 2.5 and 3.5 Å, the HOMO and LUMO become nearly degenerate and thus the energy difference between the ground and first excited state (obtained from TDDFT calculations) drops significantly. This is indicative of an avoided crossing and thus also a true barrier seems to be present for the dissociation of NH_3 from the full [HIPTN$_3$NMo](N)$^+$ complex.

The resulting [**Mo**](N)$^+$ complex (**17**) is *not* a Mo(VII) species as one might think at first sight. Population analysis (according to Löwdin) shows that the charge on molybdenum changes only by 0.002 e between [**Mo**](N) and [**Mo**](N)$^+$. Inspection of the HOMO of both the neutral and the cationic complex shows that electron density is built up only on the HIPTN$_3$N ligand and not on the central molybdenum. The positive charge is therefore smeared across the HIPTN$_3$N ligand which once again acts as a "non-innocent" ligand. Thus, **17** is truly a genuine Mo(VI)−nitride species, which is also supported by the extremly small difference in the Mo≡N bond lengths (0.14 pm) of **13** and **17**.

3.5. Transfer of the Fourth Electron/Proton Pair. Possible reaction pathways for the first reduction/protonation step of the molybdenum nitrido complex **16** are depicted in Scheme 6. Comparable to all of the previous steps, direct reduction of the [**Mo**](N) complex (**16**) to **18** is not feasible from an energetical point of view. Instead, protonation is again required prior to reduction. Transfer of a proton on either the ligand (to give **19**) or the nitride moiety (to give **20**) is an exothermic process, but protonation of the nitride is favored by more than 50 kJ mol^{-1}. Therefore, a proton transfer to the ligand is rather unlikely during this reaction step.

Scheme 6. Possible Reaction Paths for the Transfer of the First Electron and Proton onto the Mo−N Moiety[a]

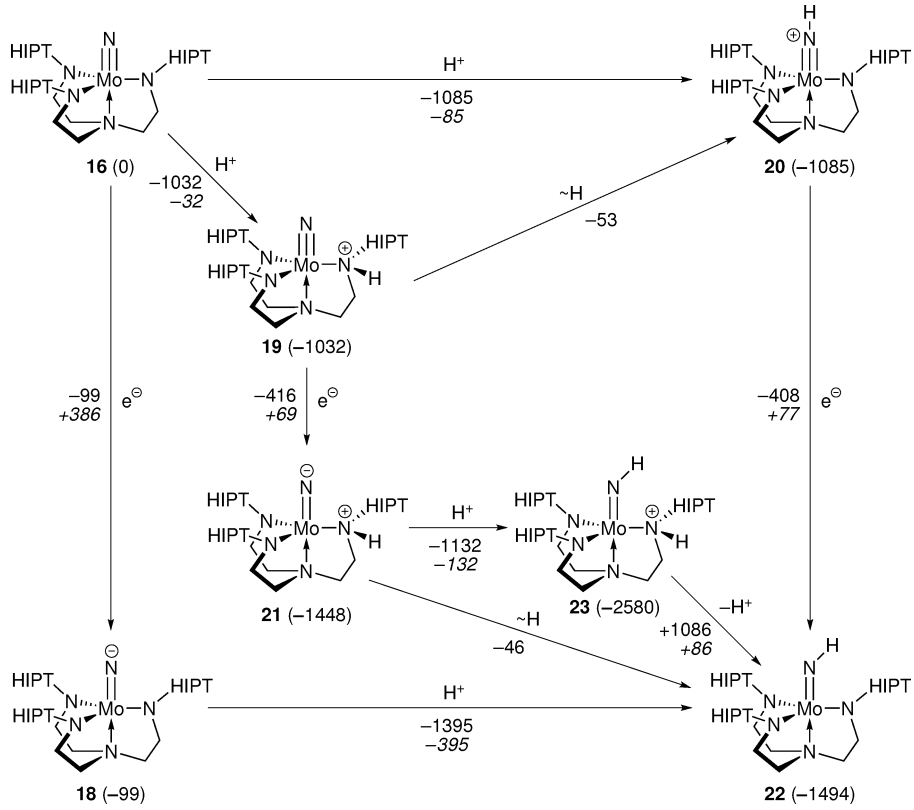

[a] Energies are given in kJ mol^{-1}. Values in *italics* correspond to the reaction energies obtained with lutidinium or Cr(cp*)$_2$, respectively.

Both the reduction of **19** to **21** and that of **20** to **22** are comparable in energy ($\Delta\Delta E = 8$ kJ mol^{-1}). Therefore, this step will not show a strong preference of one or the other reaction path. The reduced complex with protonated ligand (**21**) can easily be protonated at the terminal nitrogen atom yielding **23**. Subsequent deprotonation of the ligand is slightly endothermic and yields the [**Mo**](NH) species **22**.

As already mentioned, protonation at the ligand is disfavored by approximately 50 kJ mol^{-1}, while the subsequent steps are comparable in their energy requirements. While this difference is not large enough to completely rule out protonation of the ligand, such a mechanism, nevertheless, appears less likely. Therefore, the [**Mo**](NH) complex (**22**) is formed by protonation at the terminal nitrogen, followed by one-electron reduction without involving species where the ligand is protonated.

3.6. Transfer of the Fifth Electron/Proton Pair. Reaction paths for the transfer of the second electron and second proton onto the nitrido species are depicted in Scheme 7. Direct reduction of the neutral [**Mo**](NH) complex (**22**) to **24** is energetically unfeasible, a feature common with all previous steps. As in the previous step, protonation of the terminal nitrogen (yielding **25**) is favored over ligand protonation (yielding **23**) by more than 50 kJ mol^{-1}.

Reduction of the imino species **23** to **26** is very feasible ($\Delta E = -501$ kJ mol^{-1}). In comparison, reduction of the cationic amido complex **25** to **27** is less exothermic by more than 50 kJ mol^{-1}. The overall reaction path thus depends on the particular choice of the reducing agent. If strong reductants are applied, reduction of **25** becomes possible, and **27** is formed without the involvement of complexes with a protonated ligand nitrogen atom. If, however, the reductant is weak, an alternative route opens up. Because **25** will not be reduced, an equilibrium between the two different protonated species **25** and **23** will emerge. For thermodynamic reasons, the complex with a protonated ligand (**23**) will only be present in small amounts but can readily be reduced to **26**. Thus, the cationic complex **23** is constantly removed from the equilibrium. Protonation of the azanide **26** gives **28** and subsequent deprotonation of the ligand finally yields the [**Mo**](NH$_2$) complex (**27**).

3.7. Transfer of the Sixth Electron/Proton Pair. The possible pathways for the transfer of the last electron−proton pair are shown in Scheme 8. Reduction of the neutral [**Mo**](NH$_2$) complex to **29** is endothermic and thus almost impossible. Protonation of either the ligand (leading to **28**) or the terminal nitrogen (yielding **30**) seems to be energetically comparable ($\Delta\Delta E = 17$ kJ mol^{-1}). However, reduction of the latter one is preferred by 60 kJ mol^{-1}. Given the fact that the reduction step finally favors the reaction path involving **30**, it is apparently unlikely that any of the complexes with a protonated ligand (**28**, **31**, and **32**) plays an important role in the formation of the [**Mo**](NH$_3$) complex (**33**).

3.8. Closer Look at the Protonation Mechanism Employing a One-Pot Model. For all protonation steps discussed so far, we used an isolated molecule approach where complex and acid are treated separately at infinite distance.

Scheme 7. Possible Reaction Paths for the Transfer of the Second Electron and Proton onto the Mo−NH Moiety[a]

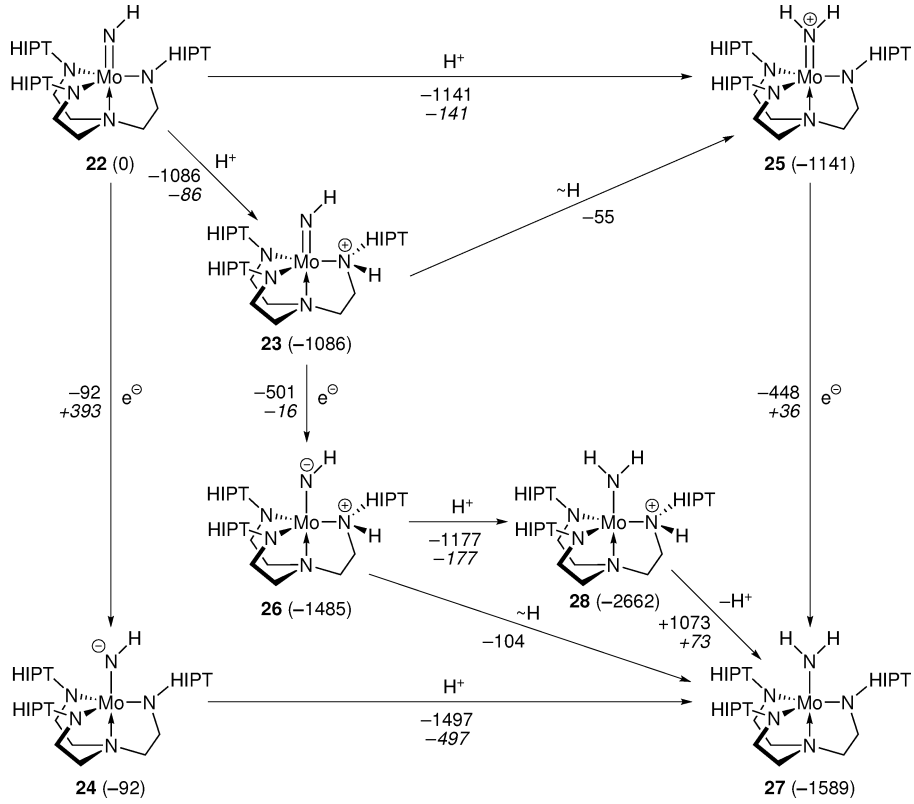

[a] Energies are given in kJ mol^{-1}. Values in *italics* correspond to the reaction energies obtained with lutidinium or Cr(cp*)$_2$, respectively.

Although this is a well established procedure, it neglects all possible acid−base interactions, apart from the fact that individual reaction energies turn out to adopt very large absolute values. Since inclusion of the latter ones may even lead to a qualitatively different picture, we checked the influence of the acid/base within a *one-pot model*.

By one-pot model, we mean that both acid and base are placed at finite distance (about 8 Å away from the nitrogen atom that will be protonated) in a supermolecule approach. Then, a structure optimization is performed. Of course, this approach is very computer time demanding (especially in view of the size of the isolated catalyst itself, which is already so large that all isolated catalyst calculations presented here can be considered to be highly nonstandard), which is the reason why it is usually not performed.

For steric reasons, protonation of the terminal N_xH_y ligand or the amide N of the HIPTN$_3$N ligand can proceed through different entrance channels toward the cage built up by the bulky HIPT substituents (Figure 1). Channel a corresponds to protonation of the N_xH_y moiety, while channel b, for which three options exist, is predestined for transfer of a proton onto the HIPTN$_3$N ligand.

The approach of lutidinium through either channel was investigated for the [**Mo**](N$_2$) (**1**) and [**Mo**](N) (**16**) complexes. The corresponding reaction energies for the different products are given in Figures 2 and 3. As can be seen from these data, the absolute values of the reaction energies do change by several 10 kJ mol^{-1} between the two different computational approaches. However, it is very important to understand that the preferred site for protonation never changes. Since it is reasonable to assume a similar behavior for all other protonation steps, the modeling error introduced by the computationally much-less demanding *isolated*-molecule approach presented above does not affect the qualitative discussion of the protonation steps. From a quantitative point of view, Figures 2 and 3 show that the isolated-molecule approach consistently leads to a slight overstabilization of the protonated complexes as one would expect.

Interestingly, we were able to locate encounter complexes for the approach of lutidinium through channel a for both **1** and **16** (Figure 4). Surprisingly, the lutidinium is sufficiently small to fit into the cavity built up by the HIPT ligand. A more bulky acid might, however, have difficulties approaching the active site. In both encounter complexes, a hydrogen bond is present between the proton to be transferred and the N$_2$ or N moiety. In the [**Mo**](N$_2$) complex, a hydrogen bond with both N$^\alpha$ and N$^\beta$ is established simultaneously. This is possible because the lutidinium is located very close to the active site. The corresponding distances of the proton to be transferred are 1.778 (N$^\beta$) and 2.850 Å (N$^\alpha$). From the calculation of shared-electron-numbers, it is evident that the bond to N$^\beta$ is roughly twice as strong (−38.9 kJ mol^{-1}) as that to N$^\alpha$ (−21.1 kJ mol^{-1}). As one might expect, in the [**Mo**](N) complex (**16**), the hydrogen bond is much stronger (−97.0 kJ mol^{-1}) and the corresponding N−H distance is quite short (1.520 Å).

Up to now, only thermodynamic aspects of the protonation reactions have been investigated. To ensure that the preferred site for protonation can really be deduced solely from

Scheme 8. Possible Reaction Paths for the Transfer of the Third Electron and Proton onto the Mo−NH_2 Moiety[a]

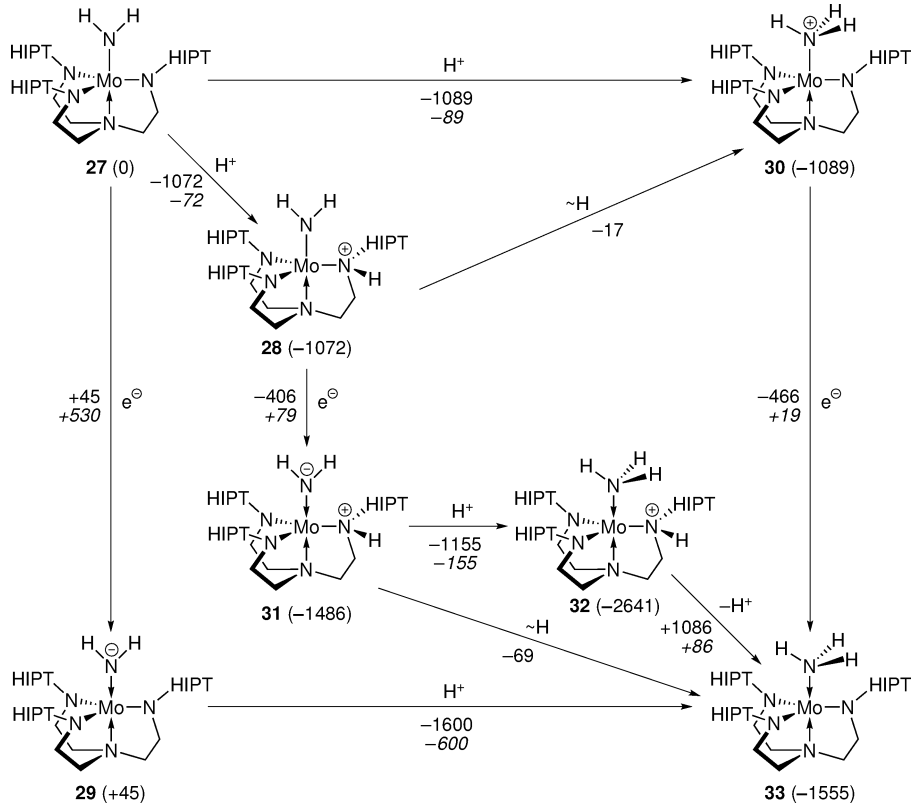

[a] Energies are given in kJ mol^{-1}. Values in *italics* correspond to the reaction energies obtained with lutidinium or $Cr(cp^*)_2$, respectively.

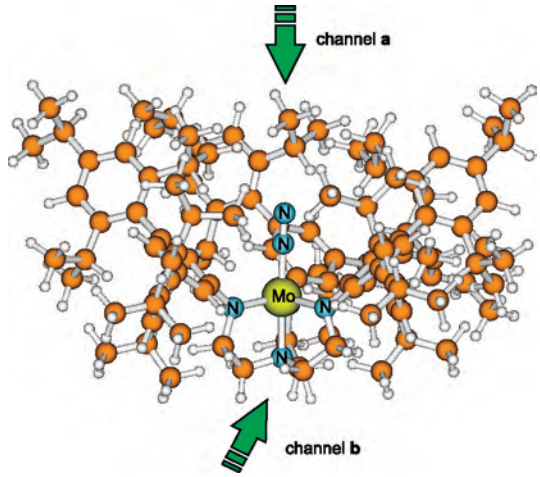

Figure 1. Two possible entrance channels for an acid to deliver a proton. Note that the complex offers three different possibilities for channel b depending on the direction from which a reactant approaches from below.

thermodynamics, we estimated the barriers for the proton transfer onto the Mo−(N≡N) and Mo≡N moieties. To this end, we calculated several points along the intrinsic reaction path leading from the encounter complexes to the corresponding products by fixing the distance between the proton and the acceptor nitrogen atom while relaxing the remaining degrees of freedom. From these calculations we can give an upper bound to the barriers of at most 20 kJ mol^{-1}. Naturally, such a barrier can be easily overcome at the reaction conditions usually applied and thus kinetic aspects are likely to play a minor role in our first attempt to an understanding of the Schrock mechanism. The small barrier heights also indicate that protonation is always reversible.

The flexibility of the three HIPT substituents of the trisamidoamine ligand was already observed experimentally by Schrock and co-workers, who were able to isolate a cationic complex where lutidinium is directly coordinated to the molybdenum and to determine its structure by X-ray crystallographic methods.[55]

3.9. Exchange of NH_3 and N_2. The exchange of the second ammonia ligand by a newly incoming dinitrogen molecule is the final step that closes the catalytic cycle. Possible mechanisms for this last step have already been explored in our previous paper.[31] Our calculations demonstrated that an NH_3/N_2 exchange in the cationic system (**30**) is unlikely for thermodynamic reasons. NH_3 can only be replaced by N_2 if the complex is at least neutral or even negatively charged (see also discussion of complexation energies below).

A weak reductant may not be able to reduce the neutral [**Mo**](NH_3) complex **33** to the anionic form (**34**) to a significant amount. If, however, reduction can be achieved, the exchange of coordinated ammonia by dinitrogen in **34** is very feasible from a thermodynamic point of view.[31]

The results depicted in Scheme 8 also show that the neutral complex **33** can be protonated at one of the ligand amide nitrogen atoms yielding **32**. It is therefore reasonable to assume that neutral **33** will only be present in small amounts because it will be either easily protonated or reduced.

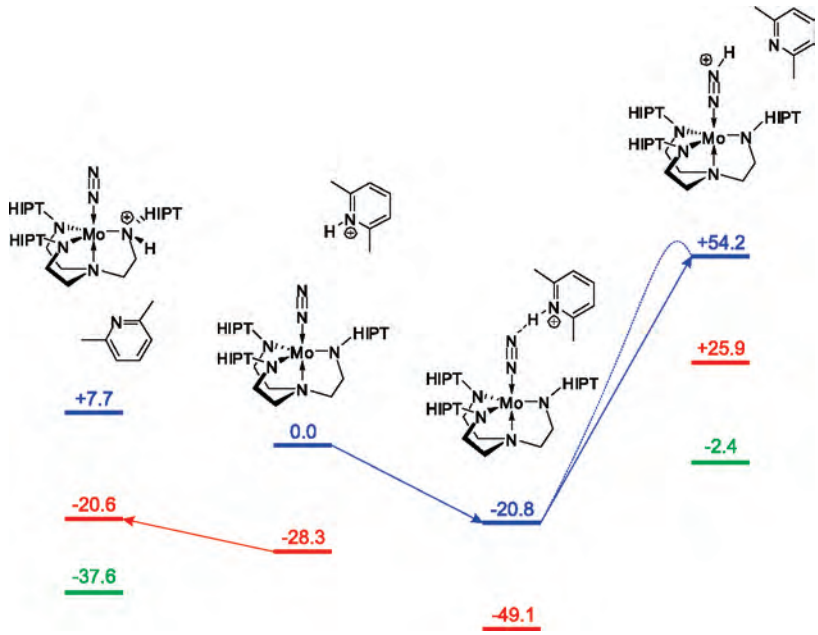

Figure 2. Energies (kJ mol^{-1}) obtained with the one-pot model for protonation of the [**Mo**](N$_2$) complex (**1**). Channel a is depicted in blue, while channel b is in red. The green values correspond to the intrinsic reaction energies ($\Delta_R E^{\text{intrinsic}}$, Scheme 2) plus the energy required to abstract the proton from lutidinium (+1000.2 kJ mol^{-1}). Note the estimated barrier indicated by a dashed line for the proton transfer step on the right-hand side.

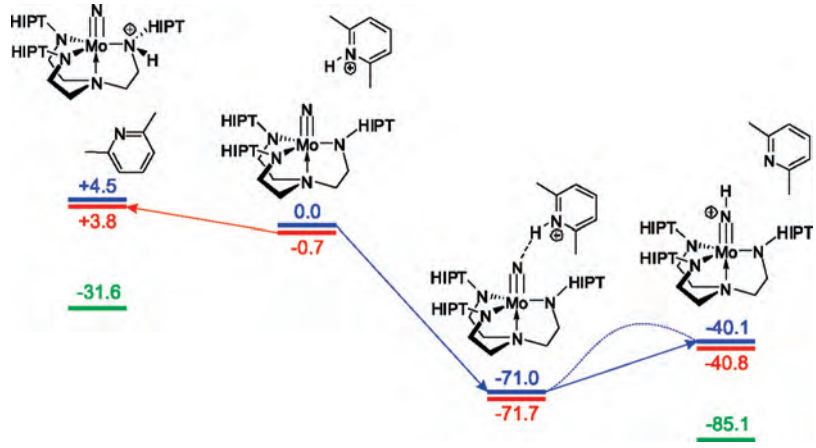

Figure 3. Energies (kJ mol^{-1}) obtained with the one-pot model for protonation of the [**Mo**](N) complex (**16**). Channel a is depicted in blue, while channel b is in red. The green values correspond to the intrinsic reaction energies ($\Delta_R E^{\text{intrinsic}}$, Scheme 6) plus the energy required to abstract the proton from lutidinium (+1000.2 kJ mol^{-1}). Note the estimated barrier indicated by a dashed line for the proton transfer step on the right-hand side.

A question which has not been addressed in our previous work is whether the exchange may involve a six-coordinate metal complex which binds both ligands simultaneously. So far we have considered only the possibility of a four-coordinate intermediate which emerges when ammonia dissociates and allows the dinitrogen ligand to approach the ligand from above.[31] Applying *first-principles* molecular dynamics simulations,[67] we observed a six-coordinate intermediate that may be important in the ligand exchange reaction.[68] From the trajectory obtained, we cut out a snapshot of a six-coordinate intermediate. Subsequent structure optimization yielded a stable intermediate depicted in Figure 5. Hence, the dinitrogen ligand may approach the catalyst from below and coordinate in the plane of the amide nitrogen atoms. A more-detailed discussion of the mechanistic details of this important step is beyond the scope of this work and will be presented elsewhere.[68]

3.10 Complexation Energies. During the catalytic cycle, several complexes are formed where small stable molecules coordinate to the molybdenum center. Table 2 provides binding energies for N_2, N_2H_2, and NH_3. Some of the data, namely, those for N_2 and NH_3, have already been published in our preceding communication.[31] The slight differences between the energies reported earlier and the present results in Table 2 are the result of re-optimization of the corresponding complexes and a different spin state of [**Mo**]$^+$ (see below).

These results show that dinitrogen is bound more strongly upon reduction of [**Mo**](N$_2$), while the bonding energy decreases upon oxidation. A (very) weak coordination of N_2 in the cationic and a strong one in the anionic complex was suggested earlier on the basis of IR measurements[23] and

(67) Thar, J.; Reckien, W.; Kirchner, B. *Top. Curr. Chem.* **2007**, *268*, 133–171.
(68) Schenk, S.; Kirchner, B.;Reiher, M. In preparation.

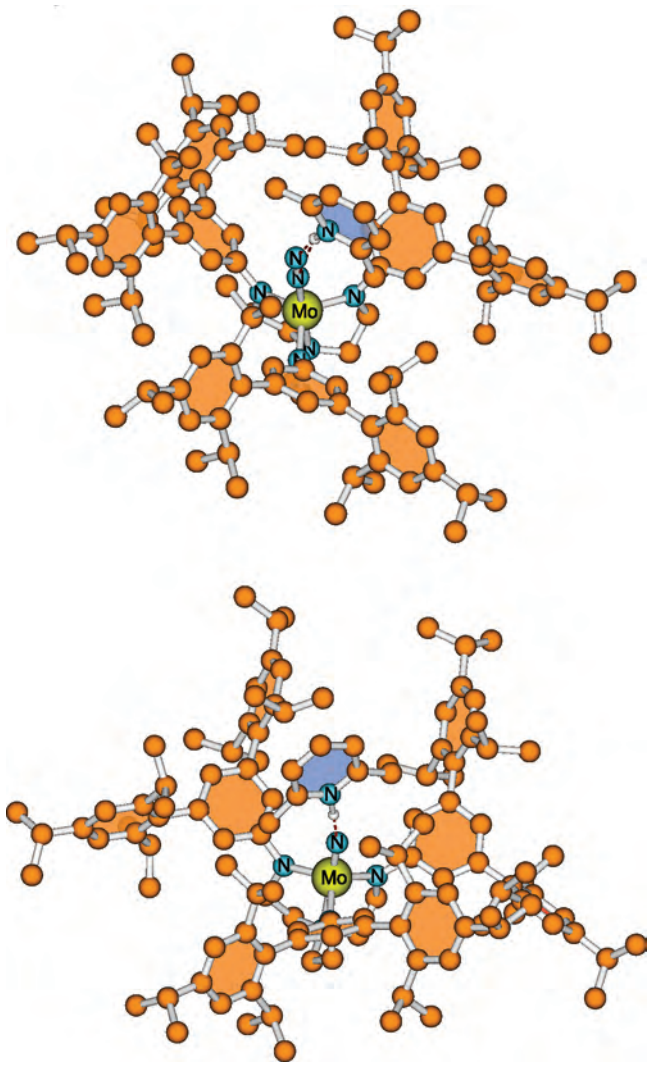

Figure 4. Graphical representation of the encounter complexes obtained by explicitely including lutidinium/lutidine as the acid/base. All carbon-bound hydrogens have been omitted for clarity. The acid is shown with a blue and the benzene rings of the terphenyl groups with an orange background.

predicted by us in ref 31. The binding energies of N_2 in complexes with a singly or doubly protonated ligand (denoted as H-[**Mo**]$(N_2)^+$ and (H,H)-[**Mo**]$(N_2)^{2+}$ in Table 2, are intermediate between those for cationic [**Mo**]$(N_2)^+$ and neutral [**Mo**](N_2).

The binding energies for NNH_2 follow the opposite trend as compared to N_2. *iso*-Diazene is bound most strongly in the cationic complex. This strong coordination is corroborated by the fact that the molecular structure of [**Mo**]$(NNH_2)^+$ (**9**) could be determined by X-Ray crystallographic analysis.[55]

Among all three different diazenes, the iso isomer binds most strongly. The energy gained upon complexation of either *trans*- ($\Delta E^{compl} = -247$ kJ mol^{-1}) or *cis*-diazene ($\Delta E^{compl} = -252$ kJ mol^{-1}) is essentially identical and by more than 100 kJ mol^{-1} smaller than that of the iso isomer **10**. This superior complexation ability of *iso*-diazene more than compensates for the unfavorable iso arrangement.

Interestingly, [**Mo**](NNH_2) (**10**) could not be observed experimentally.[55] From our calculations it is clear that a weak binding of N_2H_2 is not the reason ($\Delta E^{compl} = -354$ kJ mol^{-1}). Instead, **10** is rapidly converted into a mixture of different compounds under the reaction conditions. Schrock et al. proposed a sequence of six different reactions to take place.[55]

$$[\mathbf{Mo}](NNH_2)^+ + e^- \rightarrow [\mathbf{Mo}](NNH_2) \quad (3)$$

$$[\mathbf{Mo}](NNH_2)^+ + [\mathbf{Mo}](NNH_2) \rightarrow [\mathbf{Mo}](NNH) + [\mathbf{Mo}](NNH_3)^+ \quad (4)$$

$$[\mathbf{Mo}](NNH_3)^+ + e^- \rightarrow [\mathbf{Mo}](N) + NH_3 \quad (5)$$

$$2[\mathbf{Mo}](NNH_2)^+ + 2e^- \rightarrow [\mathbf{Mo}](NNH) + [\mathbf{Mo}](N) + NH_3 \quad (6)$$

$$5[\mathbf{Mo}](NNH_2)^+ + 4e^- \rightarrow 4[\mathbf{Mo}](NNH) + [\mathbf{Mo}](NH_3)^+ + NH_3 \quad (7)$$

$$[\mathbf{Mo}](NNH_2)^+ + e^- \rightarrow [\mathbf{Mo}](NNH) + \frac{1}{2}H_2 \quad (8)$$

Table 3 gives energetic details for all reactions. These energies demonstrate the advantage of our approach to give the intrinsic reaction energies because these are independent of a particular choice of a reductant. Their corresponding ionization energies are merely a parameter that shifts the intrinsic energy.

Reaction 6, being the net reaction of reactions 3−5, is always feasible under the reaction conditions applied. Therefore, although [**Mo**](NNH_2) (**10**) may be formed only in minute amounts because of the endothermicity of the reduction (reaction 8), it will nevertheless be readily converted into [**Mo**](N) (**16**) and ammonia. Thus, the concentration of **10** in solution will always be very small. This will make its experimental detection very difficult, if not impossible. If larger amounts of stronger reducing agents such as $Co(cp^*)_2$ are employed, reaction 7 might become competitive with reaction 6.

Formation of dihydrogen, reaction 8, always competes with reduction of **9**, reaction 3, and is found to be energetically favored by approximately 50 kJ mol^{-1} (Table 3). Indeed, with the weakest reductant $Co(cp)_2$, formation of H_2 has been experimentally observed.[55] Because reduction of **9** may be incomplete, excess reductant can react with lutidinium always present under the reaction conditions. In the experiment, acid and reductant are constantly added in small amounts to avoid larger concentrations of both and thus keeping dihydrogen production low.[21]

In the anionic [**Mo**]$(NNH_2)^-$ complex (**14**), diazene is only very weakly bound, even weaker than N_2 in [**Mo**]$(N_2)^+$ (Table 2). It might therefore be very difficult to isolate this compound.

As already mentioned in the discussion of the third electron/proton transfer, dissociation of ammonia from [**Mo**]$(NNH_3)^+$ is exothermic but has to overcome a barrier. Therefore, **13** should exist in principle, especially since we were able to locate such a structure on the potential energy surface. However, synthesis and characterization of significant amounts of this complex might well turn out to be unfeasible, especially because it cannot be easily generated

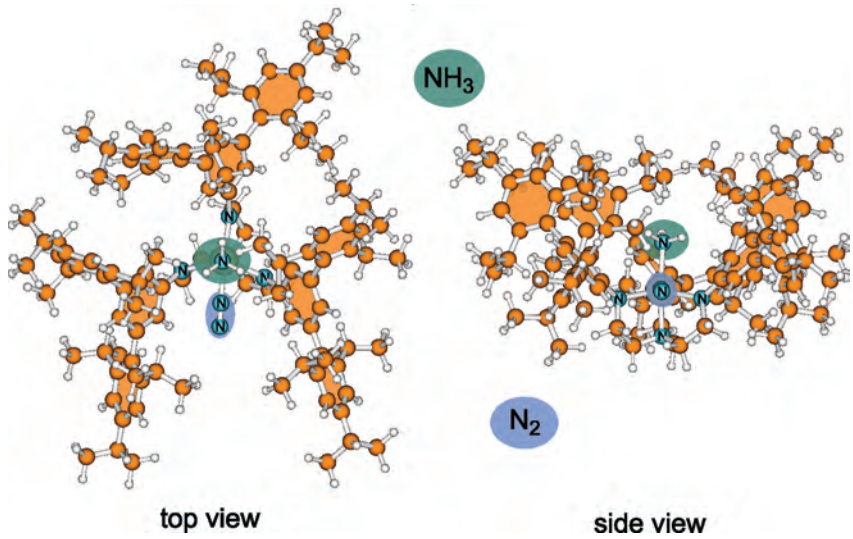

Figure 5. Stable six-coordinate intermediate of the ammonia−dinitrogen exchange reaction optimized with RI-BP86/TZVP,SVP.

Table 2. Complexation Energies, ΔE^{compl}, of Different N_xH_y Species in Complexes Involved in the Catalytic Mechanism[a]

molecule	complex	ΔE^{compl} [kJ mol^{-1}]
N_2	[**Mo**](N$_2$)$^+$	−111
	(H,H)-[**Mo**](N$_2$)$^{2+}$	−122
	H-[**Mo**](N$_2$)$^+$	−128
	[**Mo**](N$_2$)	−158
	[**Mo**](N$_2$)$^-$	−239
N_2H_2	[**Mo**](NNH$_2$)$^+$	−457
	[**Mo**](NNH$_2$)	−354
	[**Mo**](*cis*-HNNH)	−252
	[**Mo**](*trans*-HNNH)	−247
	[**Mo**](NNH$_2$)$^-$	−172
NH_3	(H,H)-[**Mo**](NH$_3$)$^{2+}$	−204
	[**Mo**](NH$_3$)$^+$	−147
	H-[**Mo**](NH$_3$)$^+$	−136
	[**Mo**](NH$_3$)	−118
	[**Mo**](NH$_3$)$^-$	−84
	[**Mo**](NNH$_3$)$^+$	+60

[a] For the diazene complexes, always the same isomer was used for the free diazene and the complex, that is, coordination of *trans*-HNNH will always result in a [**Mo**](*trans*-HNNH) complex.

Table 3. Reaction Energies, $\Delta_R E$ (kJ mol^{-1}), for Reactions 3−8[a]

reaction	$\Delta_R E^{intrinsic}$	$\Delta_R E$ {Co(cp*)$_2$}	$\Delta_R E$ {Cr(cp*)$_2$}	$\Delta_R E$ {Co(cp)$_2$}
3	−392	+48	+93	+112
4	+55			
5	−650	−210	−165	−146
6	−986	−107	−16	+22
7	−1875	−117	+65	+142
8	−445	−5	+40	+60

[a] Intrinsic ionization energies for the reductants can be found in Table 1. cp = cyclopentadiene; cp* = pentamethyl cyclopentadiene.

by protonation of [**Mo**](NNH$_2$) because the latter one is also experimentally unknown. One might be tempted to assume that it is possible to synthesize derivatives of [**Mo**](NNH$_3$)$^+$ like [**Mo**](NNH$_2$Ph)$^+$ because aniline could be a worse leaving group than ammonia and similar titanium complexes have recently been described.[69] However, an exploratory structure optimization of [**Mo**](NNH$_2$Ph)$^+$ with Ph = phenyl showed us that the opposite is the case, that is, aniline is, in the case of the Schrock catalyst, an excellent leaving group, much better than NH$_3$. The complex [**Mo**](NNH$_2$Ph)$^+$ is thus less stable with respect to dissociation than is [**Mo**](NNH$_3$)$^+$.

(69) Patel, S.; Li, Y.; Odom, A. L. *Inorg. Chem.* **2007**, *46*, 6373–6381.

The complexation energies of ammonia follow the opposite trend as those of dinitrogen. Therefore, exchange of ammonia by dinitrogen is unfeasible at a cationic molybdenum center, while it readily occurs in neutral or anionic complexes. This fact was described by us earlier.[31]

3.11 Net Reactions. The general net reaction for the transfer of one electron and one proton onto the N_xH_y moiety is given by

$$[\mathbf{Mo}](N_xH_y) + HA + Red \rightarrow [\mathbf{Mo}](N_xH_{y+1}) + A^- + Red^+ \quad (9)$$

where HA denotes the proton and Red the electron source. So far, this reaction has been split into the following steps:

$$[\mathbf{Mo}](N_xH_y) + H^+ + e^- \rightarrow [\mathbf{Mo}](N_xH_{y+1}) \quad (10)$$

$$HA \rightarrow A^- + H^+ \quad (11)$$

$$Red \rightarrow Red^+ + e^- \quad (12)$$

The net energy for reaction 9, $\Delta_R E^{net}$, is therefore given by

$$\Delta_R E^{net} = \Delta_R E^{(10)} + \Delta_R E^{(11)} + \Delta_R E^{(12)} \quad (13)$$

$$= \Delta_R E^{intrinsic} - PA - EA \quad (14)$$

where $\Delta_R E^{(n)}$ denotes the reaction energy for reaction n, PA the intrinsic proton affinity of the corresponding base A$^-$, and EA the intrinsic electron affinity of the oxidized reductant Red$^+$.

It is clear from equation 14 that no unique value for $\Delta_R E^{net}$ exists because of the dependence on the character of the acid and reductant applied. Since it is impossible to provide data for all potential acids and reductants, we follow a different approach. With the intrinsic reaction energies from Table 4, it is possible to calculate the net reaction energy $\Delta_R E^{net}$ for any combination of acid and reductant once their corresponding proton and electron affinities are known. The latter values can easily be obtained from density functional calculations.

No clear trends are visible in the intrinsic reaction energies (Table 4). Interestingly, the transfer of the first electron−proton

Table 4. Intrinsic Reaction Energies, $\Delta_R E^{intrinsic}$ (kJ mol^{-1}), for Reaction 10[a]

educt	products	$\Delta_R E^{intrinsic}$	$\Delta\Delta_R E^{intrinsic}$
[**Mo**](N$_2$)	[**Mo**](NNH)	−1548	+140
[**Mo**](NNH)	[**Mo**](NNH$_2$)	−1486	+202
[**Mo**](NNH$_2$)	[**Mo**](N) + NH$_3$	−1688	±0
[**Mo**](N)	[**Mo**](NH)	−1494	+196
[**Mo**](NH)	[**Mo**](NH$_2$)	−1589	+99
[**Mo**](NH$_2$)	[**Mo**](NH$_3$)	−1555	+133

[a] $\Delta\Delta_R E^{intrinsic}$ are given with respect to $\Delta_R E^{intrinsic}$ for the formation of the first molecule of ammonia.

pair is not the most difficult step in this sequence, although this has been found to be the case for other dinitrogen complexes (cf. refs 70 and 71). Instead, the second reduction/protonation step is the most difficult one with the fourth step being comparable in energy.

Table 5 gives $\Delta_R E^{net}$ values for some commonly used reactants. The net reaction energies in Table 5 show that with stronger reducing agents such as Co(cp*)$_2$ and Cr(cp*)$_2$, all reactions are exothermic or at least essentially thermodynamically neutral. Cobaltocene Co(cp)$_2$ and chromocene Cr(cp)$_2$ are somewhat intermediate such that some steps are exothermic, while others are slightly endothermic. However, because of an increased driving force resulting from precipitation of {M(cp)$_2$}{BAr$_4$′} under the reaction conditions, reduction with Co(cp)$_2$ is also feasible.[55] Nickelocene and ferrocene are too weak reductants to be successfully applied in dinitrogen fixation.

A comparison with the net reaction energies obtained in previous studies is provided in Table 6. Cao et al.[35] give their results with respect to ammonium and [Fe$_4$S$_4$(SEt)$_4$]$^{2-}$; thus, they are not directly comparable to the other results. Because these authors provide the energy required to abstract a proton from ammonium (+1174 kJ mol^{-1}) and an electron from [Fe$_4$S$_4$(SEt)$_4$]$^{2-}$ (+50 kJ mol^{-1}), it is possible to recalculate the reaction energies. With the help of equation 14 and the corresponding energies for lutidinium and Cr(cp*)$_2$, a correction term of 261 kJ mol^{-1} can be calculated. Thus, by addition of 261 kJ mol^{-1} to the energies given by Cao et al., one arrives at the values given in Table 6.

With the exception of Cao et al., all studies report the formation of the first molecule of ammonia to be the most exothermic and the transfer of the second proton−electron pair to be the least exothermic step. We should point out that the deviation of the data of Cao et al. is not the result of the introduction of our "correction term" because this is merely a constant added to each value. The same conclusion would be drawn on the basis of the raw data given in their paper.[35] The absolute values obtained in the latter study also differ significantly from the other results (which agree more or less with each another). We do not see a clear indication as to why such large differences exist and therefore will not discuss these results any further. We should note that the net reaction energies depend on the spin states that have been used to calculate the electron affinity for Cr(cp*)$_2$. Because we considered the energetically lower $S = 1.0/1.5$ pair (see above), all reaction energies would have to be reduced by 18 kJ mol^{-1} if the $S = 0.0/0.5$ pair were used.

All reaction steps are calculated by us to be somewhat less exothermic than those reported by other groups. The differences range from 14 kJ mol^{-1} to a whopping 108 kJ mol^{-1} but are not equally distributed. The data of Magistrato et al. (HIPT substituted by phenyl) generally show smaller and more uniform deviations of −40 ± 20 kJ mol^{-1} than that of Studt et al. (HIPT replaced by hydrogen). Any deviation in the energies for proton abstraction from the acid or electron abstraction from the reductant would lead to a constant shift in the reaction energies. Some scattering will, naturally, be introduced by the intrinsic error of the DFT method applied. The remaining sources of error are the deviations in the intrinsic reaction energies which strongly depend on the "quality" of the ligand. That is, the error with hydrogens replacing HIPT should be larger than that with phenyl groups. Exactly this behavior can be seen in Table 6 further confirming our previous findings that a simplification of the HIPT substituent leads to significantly different results for the thermodynamics of the Schrock cycle.[30,31]

Unfortunately, a further thorough analysis of Studt and Tuczek's results[36] and especially the large deviation in the reaction energy for the generation of the first molecule of ammonia is impossible because these authors do not provide enough data. However, given the really small size of the model system employed by Studt et al. and to ensure that the deviations are not caused by their use of the B3LYP functional, we recalculated all important reaction steps with HIPT replaced by hydrogen with the BP86, as well as the B3LYP functional, and the TZVP-SVP basis set used throughout this paper. These calculations show that with respect to the HIPT substituent most reaction steps are well-reproduced (independent of the functional) which might be understood as an indication that the basis sets used in ref 36 are simply too small. Only for reactions leading to formation of an ammonia molecule and the NH$_3$/N$_2$ exchange reaction did larger deviations occur.

3.12 Importance of Higher Spin States. The potential role of spin states of higher multiplicity has been previously noted by us and others.[30,36] Experimentally, only few data are available. For the [**Mo**](N$_2$) complex (**1**), it is known from ESR experiments that the state with $S = 0.5$ is the ground state.[72] Some complexes are known to be diamagnetic (**2**, **6**, **9**, **16**, and **20**) and thus should have a $S = 0$ singlet ground state.[22] Interestingly, the {[**Mo**](NH$_3$)}{BAr$_4$′} compound is found to be paramagnetic despite its even number of electrons.[22] From NMR data, it is known that for [**Mo**](NH$_2$) the singlet and triplet states are very close in energy.[55]

To investigate the possible participation of higher spin states in the catalytic cycle more thoroughly, we performed B3LYP* single-point calculations using the BP86 optimal geometries (see Computational Details). From these calculations, we find that the spin state with lowest multiplicity is

(70) Reiher, M.; Kirchner, B.; Hutter, J.; Sellmann, D.; Hess, B. A. *Chem.—Eur. J.* **2004**, *10*, 4443–4453.
(71) Kirchner, B.; Reiher, M.; Hille, A.; Hutter, J.; Hess, B. A. *Chem.—Eur. J.* **2005**, *11*, 574–583.
(72) McNaughton, R. L.; Chin, J. M.; Weare, W. W.; Schrock, R. R.; Hoffman, B. M. *J. Am. Chem. Soc.* **2007**, *129*, 3480–3481.

Table 5. Net Reaction Energies, $\Delta_R E^{net}$ (kJ mol^{-1}), Calculated with Equation 14 for Some (Commonly Applied) Metallocenes[a]

educt	products	$Co(cp^*)_2$	$Cr(cp^*)_2$	$Co(cp)_2$	$Cr(cp)_2$	$Ni(cp)_2$	$Fe(cp)_2$
[**Mo**](N_2)	[**Mo**](NNH)	−108	−63	−44	−9	+45	+100
[**Mo**](NNH)	[**Mo**](NNH_2)	−46	−1	+18	+53	+107	+163
[**Mo**](NNH_2)	[**Mo**](N) + NH_3	−249	−203	−184	−149	−95	−40
[**Mo**](N)	[**Mo**](NH)	−54	−8	+11	+46	+100	+155
[**Mo**](NH)	[**Mo**](NH_2)	−150	−105	−85	−50	+4	+60
[**Mo**](NH_2)	[**Mo**](NH_3)	−115	−69	−50	−15	+39	+94

[a] Lutidinium is always used as the acid (PA = −1000.2 kJ mol^{-1}). The electron affinities (EA) are taken from Table 1.

Table 6. Comparison of Net Reaction Energies (kJ mol^{-1}) Reported by Cao et al.,[35] Studt and Tuczek,[36] and Magistrato et al.[38] for the Reaction with Lutidinium and $Cr(cp^*)_2$[a]

educt	products	Cao et al.	Studt et al.	Magistrato et al.	this work
[**Mo**](N_2)	[**Mo**](NNH)	+68	−77	−126	−63
[**Mo**](NNH)	[**Mo**](NNH_2)	+39	−39	−41	−1
[**Mo**](NNH_2)	[**Mo**](N) + NH_3	+1	−311	−222	−203
[**Mo**](N)	[**Mo**](NH)	−57	−103	−50	−8
[**Mo**](NH)	[**Mo**](NH_2)	−67	−167	−130	−105
[**Mo**](NH_2)	[**Mo**](NH_3)	+20	−111	−113	−69
[**Mo**](NH_3)	[**Mo**](N_2)	−10	−23	−33	−41

[a] The data of Cao et al. have been corrected for these reactants (see text).

Table 7. Energy Splittings (kJ mol^{-1}) for Some Complexes Obtained from B3LYP*/TZVP-SVP Optimizations[a]

no.	compound	$S = 1.0$	$S = 1.5$
14	[**Mo**](NNH_2)$^-$	+24	
15	H-[**Mo**](NNH_2)	+9	
24	[**Mo**](NH)$^-$	−11	
26	H-[**Mo**](NH)	−23	
27	[**Mo**](NH_2)	−9	
28	H-[**Mo**](NH_2)$^+$	−20	
29	[**Mo**](NH_2)$^-$		+39
30	[**Mo**](NH_3)$^+$	−75	
31	H-[**Mo**](NH_2)		±0
32	H-[**Mo**](NH_3)$^+$		+15
36	[**Mo**]		+10
35	[**Mo**]$^+$	−56	
37	[**Mo**]$^-$	+28	
38	[**Mo**](N_2)$^+$	−31	

[a] The energy of the state with lowest multiplicity is always set to zero.

the ground state for virtually all complexes. The only exceptions are the three cationic [**Mo**]$^+$ (**35**), [**Mo**](N_2)$^+$ (**38**), and [**Mo**](NH_3)$^+$ (**30**) complexes where the triplet states ($S = 1$) are calculated to be 31.4, 5.9, and 44.9 kJ mol^{-1}, respectively, lower in energy than the singlet state ($S = 0$). All three complexes should therefore be paramagnetic. For **30**, this is confirmed by experiment.[22,23] For most of the remaining complexes, especially for those which are known from experiment to be diamagnetic, the spin state with second-lowest multiplicity is much higher in energy (>100 kJ mol^{-1}) than the lowest one. Notable exceptions of this are compounds **14**, **15**, **24**, **26**−**29**, **31**, **34**, **36**, and **37** where the energy difference between the lowest two spin states is less than 50 kJ mol^{-1}.

Because a relaxation of the structure of the latter compounds could possibly result in changes in the order of the spin states, we performed, for some of them, structure optimizations with the B3LYP* functional. Table 7 shows that, as expected, the energy difference decreases for all complexes and that for **24** and **26**−**28,** the triplet state even becomes lower in energy. For the H-[**Mo**](NH_2) complex (**31**), quartet and doublet state are essentially isoenergetic.

Table 8. Comparison of the Vertical Energy Splittings (kJ mol^{-1}) between Different Spin States of Intermediates in the Catalytic Cycle Previously Reported by Studt and Tuczek[36] with Those Obtained in the Present Work[a]

compound	S^{low}/S^{high}	Studt et al.	B3LYP*//BP86 single-point	B3LYP*//B3LYP* optimization
[**Mo**]	0.5/1.5	−0.4	+46.1	
[**Mo**](N_2)	0.5/1.5	+116.4	+182.1	
[**Mo**](NNH)	0.0/1.0	+116.8	+186.4	
[**Mo**](NNH_2)$^-$	0.0/1.0	+10.9	+31.8	+24
[**Mo**](NH_2)	0.0/1.0	−14.2	+7.5	−9
[**Mo**](NH_3)$^+$	0.0/1.0	−53.2	−44.9	−75
[**Mo**](NH_3)	0.5/1.5	+157.8	+99.3	

[a] Note that B3LYP and B3LYP* essentially give the same energetics for Schrock-type complexes (see text).

The possible participation of spin states of higher multiplicity has also been investigated by Studt and Tuczek.[36] It is not clear whether their energies are also vertical energy splittings or were obtained from a re-optimization of the geometry within the corresponding spin state. Nevertheless, it is quite interesting to compare these previous results for the model system with those from the present work (Table 8). The data from the table show that with the exception of [**Mo**](NH_3) all splittings are (severely) underestimated. The differences become smaller for [**Mo**](NNH_2)$^-$ and [**Mo**]-(NH_2) when compared to our B3LYP*//B3LYP* results. However, for [**Mo**](NH_3)$^+$, agreement is worse. Even after geometry relaxation effects are taken into account, significant deviations between our and Studt and Tuczek's results remain that may be attributed to the small basis set in ref 31 and to the replacement of the HIPT substituents by hydrogen because calculations with B3LYP on the full $HIPTN_3N$ ligand confirm the B3LYP* results. To be more specific, for [**Mo**], we obtain a vertical energy splitting of +46.1 kJ mol^{-1} with B3LYP* (see Table 8), while we obtain +45.5 kJ mol^{-1} with standard B3LYP. Accordingly, we obtained +182.1 kJ mol^{-1} for [**Mo**](N_2) with B3LYP* (see Table 8) and +179.3 kJ mol^{-1} with B3LYP, respectively. The same agreement between B3LYP* and standard B3LYP was observed for [**Mo**](NNH) (+186.4 kJ mol^{-1} with B3LYP* and +177.6 kJ mol^{-1} with B3LYP) and for [**Mo**](NH_3)$^+$ (−44.9 kJ mol^{-1} with B3LYP* and −49.2 kJ mol^{-1} with B3LYP), respectively. The dependence of the energy splitting on the exact exchange admixture in the functional has thus a very small slope (see for other examples ref 46), and hence, B3LYP and B3LYP* give very similar results in the case of Schrock's catalyst.

In summary, the changes in the reaction energies caused by the participation of spin states with higher multiplicity are quite small and never lead to preference of an alternative reaction path. Thus, the qualitative picture shown so far and the conclusions drawn remain unchanged.

4. Conclusions

In the present study, we investigated the full catalytic cycle of dinitrogen fixation by $HIPTN_3NMo$ ([**Mo**]) employing the full HIPT substituent. By reporting the intrinsic reaction energies for each protonation/reduction step, we provide a powerful tool which allows the prediction of whether, for a certain combination of acid and reductant, reduction of dinitrogen is thermodynamically feasible. We have been able to show that in every step the corresponding complex must be protonated prior to reduction for simple thermodynamic reasons. The intrinsic reaction energies for the reduction of the [**Mo**](N_xH_y) complexes do follow a trend. With increasing number of hydrogens, the reaction becomes less exothermic and, for $y = 2$, even endothermic. The energetically most difficult step is the transfer of the second electron and proton pair, while formation of the first molecule of ammonia is the most feasible one.

For the first time, alternative routes for the proton transfer have also been investigated, and we found that protonation of the ligand is feasible and sometimes even preferred. For the [**Mo**](N_2) and [**Mo**](NNH_2) complexes, the preferred site of protonation is one of the amide nitrogen atoms of the trisamidoamine chelate ligand. Thus, $HIPTN_3N$ clearly acts as a "non-innocent" ligand during the generation of the first molecule of ammonia. One may therefore speak of a "proton-catalyzed reductive protonation".[6] For the second half of the catalytic cycle, that is, the reductive protonation of [**Mo**](N), the proton is exclusively transferred onto the NH_x moiety because it is much more basic than the ligand's amide nitrogen atoms. During the investigation of the protonation steps, we also found that an explicit consideration of the acid/base using a one-pot model does not lead to significant changes in the reaction energies, and one can therefore rely on the isolated molecule approach.

The dissociation energies of several complexes have been discussed. We have been able to show that for some compounds it might prove very difficult to characterize them experimentally. Most notably, we found that the [**Mo**]-$(NNH_3)^+$ complex (**13**) should exist in principle but will extremely easily loose ammonia: a fact that has been overlooked in all previous studies. This has also consequences for the catalytic mechanism. If **13** is formed, it should release ammonia not only upon reduction but may dissociate from the cationic metal fragment even in the absence of a reductant. The positive charge in the resulting [**Mo**]$(N)^+$ fragment is not located on the Mo≡N moiety but on the $HIPTN_3N$ ligand, which is therefore redox−non-innocent.

From the comparison of our data with the previously published results on much smaller model systems of the HIPT ligand, we found that such simplifications lead to sometimes substantial errors of the order of 100 kJ mol^{-1}. It must thus be emphasized that for a thorough computational investigation of the catalytic reduction of dinitrogen such simplifications are to be considered with great care because failure of a model approach for only a single step in a reaction cascade nevertheless renders it unsuitable for a general investigation of that particular reaction series.

An aspect to complete the picture presented here is the question of all barriers and kinetic effects. In this work, we estimated the barriers of two selected protonation reactions from minimum energy reaction path calculations and found them to be small. However, because of the complex structure of the HIPT substituent it is clear that theoretical mechanistic studies should not solely rely on transition states of generic model complexes. The simple transition state picture might be replaced by a molecular-dynamical one that allows us to study different reaction routes in great detail. Therefore, subsequent work currently carried out in our laboratory utilizes Car−Parrinello molecular dynamics simulations. A first study[68] will be concerned with the delicate and intriguing details of the ammonia−dinitrogen exchange step that closes the catalytic cycle. Preliminary results indicate that a six-coordinate intermediate is formed where both N_2 and NH_3 are bound in a distorted octahedral fashion as discussed above. It turns out that the $HIPTN_3N$ ligand is flexible enough to accommodate a sixth ligand.

Acknowledgment. The authors thank the Schweizer Nationalfonds SNF (Project no. 200021-113479/1) for financial support.

Supporting Information Available: Cartesian coordinates of all calculated molecules. This material is available free of charge via the Internet at http://pubs.acs.org.

IC702083P